Inorg. Chem. **2005**, *44*, 4077–4085

New Structural Motifs, Unusual Quenching of the Emission, and Second Harmonic Generation of Copper(I) Iodide Polymeric or Oligomeric Adducts with *Para*-Substituted Pyridines or *trans*-Stilbazoles

Elena Cariati,*,† Dominique Roberto,† Renato Ugo,† Peter C. Ford,‡ Simona Galli,*,§ and Angelo Sironi||

Dipartimento di Chimica Inorganica Metallorganica e Analitica, Università degli Studi di Milano, Centro di Eccellenza CIMAINA, UdR di Milano dell'INSTM and Istituto di Scienze e Tecnologie Molecolari del CNR (ISTM-CNR), Via Venezian 21, I-20133 Milano, Italy, Department of Chemistry, University of Santa Barbara, Santa Barbara, California 93106, Dipartimento di Scienze Chimiche e Ambientali, Università degli Studi dell'Insubria, Via Valleggio 11, I-22100 Como, Italy, and Dipartimento di Chimica Strutturale e Stereochimica Inorganica, Università degli Studi di Milano, Centro di Eccellenza CIMAINA, UdR di Milano dell'INSTM and Istituto di Scienze e Tecnologie Molecolari del CNR (ISTM-CNR), Via Venezian 21, I-20133 Milano, Italy

Received January 28, 2005

The structural, emissive, and nonlinear optical properties of new CuI adducts with *para*-substituted *trans*-stilbazolic and pyridinic ligands are reported. Single-crystal X-ray diffraction results indicate that the *para*-substituent on the organic ligand greatly influences the structural motif by its steric (*tert*-butyl), electronic/steric (dimethylamino), or bridging-donor (cyano) properties so that two absolutely new structural motifs, polymeric and oligomeric, are found when *trans*-stilbazole and pyridine carry a dimethylamino group in the *para*-position. In addition, a surprising photoemission behavior is observed, being the solid-state emission of [CuI(*trans*-4-stilbazole)]$_n$, [CuI(*trans*-4′-(dimethylamino)-4-stilbazole)]$_n$, and [CuI(4′-*tert*-butyl-4-stilbazole)]$_n$ totally quenched. In the case of the noncentrosymmetric CuI adduct of *trans*-4′-(dimethylamino)stilbazole a discrete second harmonic generation (SHG) occurs.

Introduction

During the past decade, interest for new materials exhibiting worthwhile photoluminescence and nonlinear optical (NLO) properties has been focused on crystalline inorganic−organic hybrids, capable of merging the advantages of the organic compounds (appreciable response speed and intensity in a wide spectral range, straightforward synthetic approach) to those of the inorganic ones (chemical, thermal, and mechanical stabilities).[1] Among the inorganic−organic hybrid materials, the adducts between group 11 metal halides (MX, with X = Cl, Br, or I) and monohapto Lewis bases with a pseudoaromatic donor nitrogen atom (L) are particularly intriguing for both the variety of structural motifs and the related optical emission displayed.[2]

We have recently investigated the photoemission and the second-order NLO properties of a series of known, noncentrosymmetric [CuX(L)]$_n$ single-stranded "chains" and double-stranded "stairs" species, namely [CuCl(quinoline)]$_n$, [CuCl(2-methylquinoline)]$_n$, [CuBr(pyridine)]$_n$, [CuBr(2,4,6-trimethylpyridine)]$_n$, [CuBr(2-methylquinoline)]$_n$, and [CuI(2,4,6-trimethylpyridine)]$_n$.[3] Solid-state emissive properties of chains were explored for the first time, while those of stairs were added to the few already studied in the literature ([CuI(pyridine)]$_n$, [CuI(3-methylpyridine)]$_n$, and [CuI(4-methylpyridine)]$_n$).[2,4] For all compounds, the high-energy (HE) emissions observed were retraced to a triplet halide-to-ligand charge transfer [^{3}XLCT*, $p_X \rightarrow \pi^*_L$] excited state

* Authors to whom correspondence should be addressed. E-mail: simona.galli@uninsubria.it (S.G.).
† Dipartimento di Chimica Inorganica Metallorganica e Analitica, Università degli Studi di Milano.
‡ Department of Chemistry, University of Santa Barbara.
§ Dipartimento di Scienze Chimiche e Ambientali, Università degli Studi dell'Insubria.
|| Dipartimento di Chimica Strutturale e Stereochimica Inorganica, Università degli Studi di Milano.

(1) See e.g.: (a) Di Bella, S. *Chem. Soc. Rev.* **2001**, *30*, 355. (b) Lacroix, P. G. *Chem. Mater.* **2001**, *13*, 3495.
(2) Ford, P. C.; Cariati, E.; Bourassa, J. *Chem. Rev.* **1999**, *99*, 3625 and references therein.
(3) Cariati, E.; Roberto, D.; Ugo, R.; Ford, P. C.; Galli, S.; Sironi, A. *Chem. Mater.* **2002**, *14*, 5116.
(4) Cariati, E.; Xianhui Bu; Ford, P. C. *Chem. Mater.* **2000**, *12*, 3385.

10.1021/ic050143s CCC: $30.25
Published on Web 05/05/2005

Chart 1

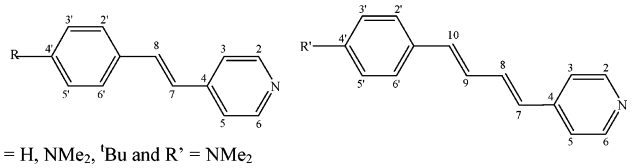

R = H, NMe_2, ^tBu and R' = NMe_2

(ES), their energy being influenced by both the polarizability of the halides and the electronic properties of the nitrogen donor ligands. Moreover, we have tested their solid-state second-order NLO activities, proving evidence for a correlation between the latter and the structural motif, stairs always showing a better response than chains.[3]

Among monohapto Lewis bases with a nitrogen donor in a pseudoaromatic system, *trans*-4-stilbazoles *para*-substituted with electron donor groups have been extensively investigated for their significant second-order NLO activities, either as metal complexes[5] or as salts, these latter particularly in the solid state.[6]

We have thus decided to pursue the investigation of solid-state photoemissive and second-order NLO responses of new CuI adducts with either *trans*-4-stilbazoles, having either a sterically demanding (*tert*-butyl) or a strong electron-donor (dimethylamino) group in position 4′, or the corresponding *para*-substituted pyridines. The more extended π-conjugation of *trans*-4-stilbazolic ligands with respect to pyridines allows one to judge the importance of π-conjugation length on the photophysical emission properties of these adducts.

In the following, we thus report on the structural, unusual lack of emission, and, when available, second-order NLO features of new CuI adducts with (see Chart 1) *trans*-4-stilbazole (**1**), *trans*-4′-(dimethylamino)-4-stilbazole (**2**), 4-*tert*-butylpyridine (**3**), and 4-(dimethylamino)pyridine (**4**). Other adducts of CuI with *trans*-4′-*tert*-butyl-4-stilbazole (**5**) and *trans*-4-[4-(4-(dimethylamino)phenyl)buta-1,3-dienyl]-pyridine (**6**), as well as of CuCl (**7**) and CuBr (**8**) with *trans*-4′-(dimethylamino)-4-stilbazole, were investigated for their emissive and second-order NLO properties only, since we were unable to obtain suitable single crystals for an X-ray structural characterization.

Experimental Section

General Comments. [CuI(pyridine)]$_4$,[7] *trans*-4′-*tert*-butyl-4-stilbazole,[8] and *trans*-4-[4-(4-(dimethylamino)phenyl)buta-1,3-dienyl]pyridine[5] were prepared according to the literature. *trans*-4-Stilbazole and *trans*-4′-(dimethylamino)-4-stilbazole were purchased from Eastman Organic Chemicals and Sigma-Aldrich, respectively, and used without further purification. All complexes were characterized by ^{1}H NMR (Bruker AC-200 and a Bruker Avance DRX 300 spectrometers) and elemental analyses carried out in the Dipartimento di Chimica Inorganica Metallorganica ed Analitica of the University of Milano.

For the numbering used in the attribution of the ^{1}H NMR signals, see Chart 1.

Synthesis and Characterization of Compounds 1−8. Synthesis of [CuI(*trans*-4-stilbazole)]$_n$ (1). A 0.153 g (0.844 mmol) amount of *trans*-4-stilbazole dissolved in 10 mL of CH_2Cl_2 was added under stirring to a solution of 0.196 g (0.182 mmol) of [CuI(pyridine)]$_4$ in 25 mL of CH_2Cl_2. A yellow solid separated, which was filtered out and washed twice with 10 mL of CH_2Cl_2 (yield 82.7%). ^{1}H NMR (CD_3CN, 25 °C): δ (ppm) 8.57 (AA′BB′, 2H, H_2, and H_6, broad), 7.63 (2 H, $H_{2'}$, and $H_{6'}$), 7.50 (d, 1 H, H_8, J = 16.2 Hz), 7.50 (AA′BB′, 2 H, H_3, and H_5), 7.45 (1H, $H_{4'}$), 7.40 (2 H, $H_{3'}$, and $H_{5'}$), 7.21 (d, 1 H, H_7, J = 16.2 Hz). Anal. Calcd for $C_{13}H_{11}$-NCuI: C, 42.00; H, 2.96; N, 3.77. Found: C, 41.34; H, 3.18; N, 3.73. Crystals of **1** suitable for X-ray diffraction were obtained by dissolution in boiling CH_3CN followed by slow cooling to room temperature and then 0 °C.

Synthesis of [CuI(*trans*-4′-(dimethylamino)-4-stilbazole)]$_n$ (2). A 0.195 g (0.872 mmol) amount of *trans*-4′-(dimethylamino)-4-stilbazole dissolved in 20 mL of CH_2Cl_2 was added under stirring to a solution of 0.202 g (0.187 mmol) of [CuI(pyridine)]$_4$ dissolved in 25 mL of CH_2Cl_2. A yellow solid separated, which was filtered out and washed twice with 10 mL of CH_2Cl_2 (yield 76%). ^{1}H NMR (CD_3CN, 25 °C): δ (ppm) 8.51 (AA′BB′, 2H, H_2, and H_6, broad), 7.51 (AA′BB′, 2 H, $H_{2'}$, and $H_{6'}$, J = 8.9 Hz), 7.43 (AA′BB′, 2 H, H_3, and H_5, J = 5.4 Hz), 7.40 (d, 1 H, H_8, J = 16.2 Hz), 6.95 (d, 1 H, H_7, J = 16.1 Hz), 6.81 (AA′BB′, 2 H, $H_{3'}$, and $H_{5'}$, J = 8.9 Hz), 3.00 (s, 6 H, NMe_2). Anal. Calcd for $C_{15}H_{16}N_2CuI$: C, 43.43; H, 3.86; N, 6.76. Found: C, 43.40; H, 3.55; N, 6.53. Rather small crystalline needles of **2**, poorly suitable for X-ray diffraction, were obtained by dissolution in hot CH_3CN followed by slow cooling to room temperature and then 0 °C.

Synthesis of [CuI(4-tert-butylpiridine)]$_4$ (3). Compound **3** was prepared by dissolving 0.314 g (1.65 mmol) of CuI in an aqueous solution saturated with KI and adding, under stirring, 0.28 mL (0.2582 g, 1.91 mmol) of 4-*tert*-butylpiridine. A white solid separated, which was washed with 12 mL of an aqueous solution saturated with KI, 20 mL of distilled water, 15 mL of methanol, and 10 mL of *n*-hexane (yield 78.8%). The tetrameric nature of compound **3** was suggested by its yellow-orange emission[4] by irradiation with a UV lamp emitting at 266 nm. By the addition of 20 mL of methanol to the reaction mother liquor, an additional amount of white solid (yield 13.7%) was obtained, which, by irradiation with the UV lamp, showed both a yellow-orange and a blue emission, suggesting the presence of both a tetrameric and a polymeric species,[4] respectively. ^{1}H NMR (($CD_3)_2CO$, 25 °C): δ (ppm) 8.90 (AA′BB′, 2H, H_2, and H_6, broad), 7.66 (AA′BB′, 2 H, H_3, and H_5, broad), 1.38 (s, 9 H, *t*-Bu). ^{1}H NMR (($CD_3)_2CO$, −80 °C): δ (ppm) 8.80 (AA′BB′, 2H, H_2, and H_6, J = 5.2), 7.72 (AA′BB′, 2 H, H_3, and H_5, J = 5.2), 1.35 (s, 9 H, *t*-Bu). Anal. Calcd for C_9H_{13}NCuI: C, 33.18; H, 3.99; N, 4.30. Found: C, 33.60; H, 3.98; N, 4.24. Crystals of **3** suitable for X-ray diffraction were obtained by addition of methanol to a CH_2Cl_2 solution of the compound.

Synthesis of [CuI(4-(dimethylamino)pyridine)]$_6$ (4). A 0.162 g (0.150 mmol) amount of [CuI(pyridine)]$_4$ was dissolved in 20 mL of CH_2Cl_2; 0.085 g (0.696 mmol) of 4-(dimethylamino)pyridine, dissolved in 3 mL of CH_2Cl_2, was then added. The solution was concentrated under vacuum up to 5−6 mL, and then 30 mL of *n*-pentane was added. The white-greenish precipitate (73.4% yield) was filtered out, washed with *n*-pentane (50 mL), and dried under

(5) See e.g.: (a) Kanis, D. R.; Lacroix, P. G.; Ratner, M. A.; Marks, T. J. *J. Am. Chem. Soc*. **1994**, *116*, 10089. (b) Roberto, D.; Ugo, R.; Bruni, S.; Cariati, E.; Cariati, F.; Fantucci, P.; Invernizzi, I.; Quici, S.; Ledoux, I.; Zyss, J. *Organometallics* **2000**, *19*, 1775.
(6) (a) Marder, S. R.; Perry, J. W.; Yakymyshyn, C. P. *Chem. Mater*. **1994**, *6*, 1137. (b) Coradin, T.; Clément, R.; Lacroix, P. G.; Nakatani, K. *Chem. Mater*. **1996**, *8*, 2153. (c) Bénard, S.; Yu, P.; Audière, J. P.; Rivière, E.; Clément, R.; Guilhem, J.; Tchertanov, L.; Nakatani, K. *J. Am. Chem. Soc.* **2000**, *122*, 9444.
(7) Malik, A. U. *J. Inorg. Nucl. Chem* **1967**, *29*, 2106.
(8) Lucenti, E.; Cariati, E.; Dragonetti, C.; Manassero, L.; Tessore, F. *Organometallics* **2004**, *23*, 687.

vacuum. The solid showed an orange emission by irradiation with a UV lamp emitting at 266 nm. ^{1}H NMR ($(CD_3)_2CO$, 25 °C): δ (ppm) 8.14 (AA′BB′, 2H, H_2, and H_6, J = 7.8 Hz), 7.16 (AA′BB′, 2 H, H_3, and H_5, J = 7.8 Hz), 3.38 (s, 6 H, NMe_2). Anal. Calcd for $C_7H_{10}N_2CuI$: C, 26.88; H, 3.20; N, 8.96. Found: C, 26.50; H, 3.15; N, 9.05. Crystals of **4** suitable for X-ray diffraction were obtained by slow diffusion of *n*-pentane in a CH_2Cl_2 solution of the compound.

Synthesis of [CuI(*trans*-4′-tert-butyl-4-stilbazole)]$_n$ (5). A 0.099 g (0.42 mmol) amount of *trans*-4′-*tert*-butyl-4-stilbazole dissolved in 20 mL of CH_2Cl_2 was added under stirring to a solution of 0.095 g (0.088 mmol) of $[CuI(pyridine)]_4$ dissolved in 20 mL of CH_2Cl_2. A yellow solid separated from the deep yellow solution by addition of an excess of *n*-pentane (yield 93%). ^{1}H NMR (CD_3CN, 25 °C): δ (ppm) 8.91 (AA′BB′, 2H, H_2, and H_6, broad), 7.52 (AA′BB′, 2 H, $H_{2'}$, and $H_{6'}$, J = 8.4 Hz), 7.44 (2 H, $H_{3'}$, and $H_{5'}$, J = 8.4 Hz), 7.36 (d, 1 H, H_8, J = 16.3 Hz), 7.31 (AA′BB′, 2 H, H_3, and H_5, J = 8.2 Hz), 7.03 (d, 1 H, H_7, J = 16.3 Hz), 1.36 (s, 9H, *t*-Bu). Anal. Calcd for $C_{17}H_{19}NCuI$: C, 47.72; H, 4.44; N, 3.27. Found: C, 47.70; H, 4.58; N, 3.36.

Synthesis of [CuI(*trans*-4-[4-(4-(dimethylamino)phenyl)buta-1,3-dienyl]pyridine)]$_n$ (6). A 0.087 g (0.35 mmol) amount of *trans*-4-[4-(4-(dimethylamino)phenyl)buta-1,3-dienyl]pyridine dissolved in 10 mL of CH_2Cl_2 was added under stirring to a solution of 0.094 g (0.087 mmol) of $[CuI(pyridine)]_4$ in 20 mL of CH_2Cl_2. An orange solid separated, which was filtered out and washed twice with 10 mL of CH_2Cl_2 (yield 71%). ^{1}H NMR (CD_3CN, 25 °C): δ (ppm) 8.5 (AA′BB′, 2H, H_2, and H_6, broad), 7.39 (4 H, H_3, H_5, $H_{2'}$, and $H_{6'}$), 7.27 (1 H, H_8), 6.87 (1 H, H_9), 6.80 (3 H, H_7, $H_{3'}$, and $H_{5'}$), 6.60 (d, 1 H, H_{10}, J = 15,3 Hz), 3.00 (s, 6 H, NMe_2). Anal. Calcd for $C_{17}H_{18}N_2CuI$: C, 46.32; H, 4.09; N, 6.36. Found: C, 45.90; H, 4.20; N, 6.55.

Synthesis of [CuCl(*trans*-4′-(dimethylamino)-4-stilbazole)]$_n$ (7). A 0.106 g (1.07 mmol) amount of CuCl was added under nitrogen atmosphere to 50 mL of saturated KCl aqueous solution. The suspension was kept under stirring up to the complete dissolution of CuCl. A 0.2 mL (0.196 g, 2.478 mmol) volume of pyridine was slowly added under a flux of nitrogen. $[CuCl(pyridine)]_4$ separated as white solid. After the mixture was filtered, the compound was washed with 10 mL of saturated KCl aqueous solution, 10 mL of methanol, and 10 mL of *n*-hexane (yield 86%). A 0.059 g (0.083 mmol) amount of this white solid was dissolved under nitrogen in 20 mL of CH_2Cl_2. With working being done under a flux of nitrogen, 0.088 g (0.395 mmol) of *trans*-4′-(dimethylamino)-4-stilbazole dissolved in 10 mL of CH_2Cl_2 was added. A yellow solid separated, which was filtered out under nitrogen (yield 86.3%). The solid must be kept and manipulated under nitrogen to avoid easy oxidation by air. Due to the compound instability to oxidation to paramagnetic species of Cu(II), the ^{1}H NMR characterization could not be performed. Anal. Calcd for $C_{15}H_{16}N_2CuCl$: C, 55.67; H, 4.95; N, 8.66. Found: C, 55.70; H, 5.05; N, 8.78.

Synthesis of [CuBr(*trans*-4′-(dimethylamino)-4-stilbazole)]$_n$ (8). A 0.11 g (0.772 mmol) amount of CuBr was added under nitrogen atmosphere to 50 mL of saturated KBr aqueous solution. The suspension was kept under stirring up to the complete dissolution of CuBr. Under a flux of nitrogen, 0.1 mL (0.098 g, 1.244 mmol) of pyridine was slowly added. $[CuBr(pyridine)]_4$ separated as white solid. After the mixture was filtered under nitrogen, the compound was washed with 10 mL of saturated KBr aqueous solution, 10 mL of distilled water, and 10 mL of *n*-hexane (yield 89.6%). A 0.096 g (0.108 mmol) amount of this white solid was dissolved under nitrogen in 20 mL of CH_2Cl_2, and then a solution of 0.164 g (0.159 mmol) of *trans*-4′-(dimethylamino)-4-stilbazole dissolved in 20 mL of CH_2Cl_2 was added. A yellow solid separated, which was filtered out under nitrogen (yield 83.5%). ^{1}H NMR (CD_3CN, 25 °C): δ (ppm) 8.86 (AA′BB′, 2H, H_2, and H_6, broad), 7.58 (AA′BB′, 2 H, $H_{2'}$, and $H_{6'}$, broad), 7.51 (AA′BB′, 2 H, H_3, and H_5, J = 8.6 Hz), 7.42 (d, 1 H, H_8, J = 16.4 Hz), 6.94 (d, 1 H, H_7, J = 16.4 Hz), 6.81 (AA′BB′, 2 H, $H_{3'}$, and $H_{5'}$, J = 6.9 Hz), 3.01 (s, 6 H, NMe_2). Anal. Calcd for $C_{15}H_{16}N_2CuBr$: C, 48.98; H, 4.35; N, 7.62. Found: C, 48.70; H, 4.51; N, 7.99. The compound can be recrystallized under nitrogen by dissolution under reflux in CH_3CN, followed by slow cooling to 0 °C. It must be kept and manipulated under nitrogen to avoid easy oxidation by air.

Photoluminescence Measurements. Solid state and solution emission spectra were recorded using a Spex Florolog 2 spectrofluorometer equipped with a Hamamatsu R 928 A water-cooled photomultiplier tube. The purity of the batches of compounds **1**−**4** used to record the spectra was assessed by checking the agreement between their XRPD diffractograms and those calculated on the basis of the single-crystal results.

Second-Order NLO Kurtz−Perry[9] Measurements. The 1064 nm wavelength of a Nd:YAG pulsed laser beam was directed on sample-containing capillaries. The scattered radiation was collected by an elliptical mirror, filtered to select only the second-order contribution, and recollected with a Hamamatsu R 5108 photomultiplier tube. SHG efficiency was evaluated by taking as reference the SHG signal of quartz.

X-ray Data Collection and Solution for Compounds 1−4. Suitable crystals were mounted in air on the glass fiber tip of a goniometer head. Data collections were performed at room temperature with a Bruker AXS SMART CCD area-detector diffractometer using graphite-monochromatized Mo Kα radiation (λ = 0.710 73 Å). A total of 2000 (**1**), 2400 (**2** and **3**), or 1800 (**4**) frames was acquired by applying the ω-scan method, with $\Delta\omega$ = 0.3°, t = 30 (**1**, **3**, and **4**) or 45 (**2**) s/frame, and sample−detector distance fixed at 3.93 (**1**), 5.52 (**2**), 4.98 (**3**), or 3.95 (**4**) cm. The first 50 frames were recollected at the end of each measurement: crystal decay was never observed. An empirical absorption correction was applied to the integrated reflections.[10] The structures were solved by direct methods[11] and successfully refined with full-matrix least squares calculations.[12] Anisotropic temperature factors were assigned to all non-disordered atoms but hydrogens, which were made riding their parent atoms with a common isotropic displacement parameter.

Since **2** is almost insoluble in the most common organic solvents, many recrystallization attempts invariably yielded small needles of rather modest quality. Lowering the temperature to 193 K resulted in no significant improvements in data collection, so that the room-temperature acquisition was definitely retained. Due to the poor data quality, difficulties were encountered in assigning the correct space group, a few orthorhombic choices being equally probable. As both the *E*-statistics and (particularly) the SHG results (see below) prompted a noncentrosymmetric crystal packing, structure solution was carried on in $Pna2_1$. The conventional figures of merit obtained from the subsequent refinement were not completely satisfactory, so that reconsideration of the space group

(9) Kurtz, S. K.; Perry, T. T. *J. Appl. Phys.* **1968**, *39*, 3798.
(10) Sheldrick, G. M. *SADABS: program for empirical absorption correction*; University of Göttingen: Göttingen, Germany, 1996.
(11) Altomare, A.; Cascarano, G.; Giacovazzo, C.; Gagliardi, A.; Moliterni, A. G. G.; Burla, M. C.; Polidori, G.; Cavalli, M.; Spagna, R. *SIR97: package for structure solution by direct methods*; 1997.
(12) Sheldrick, G. M. *SHELX97*: *program for crystal structure refinement*; University of Göttingen: Göttingen, Germany, 1997.

Table 1. Crystallographic Data and Refinement Details for Compounds **1**−**4**[a]

	1	**2**	**3**	**4**
formula	$C_{13}H_{11}CuIN$	$C_{30}H_{32}Cu_2I_2N_4$	$C_{36}H_{52}Cu_4I_4N_4$	$C_{21}H_{30}Cu_3I_3N_6$
fw	371.67	829.48	1307.72	937.83
cryst system	monoclinic	orthorhombic	orthorhombic	monoclinic
space group	$P2_1/c$	$Pna2_1$	$Pbcn$	$P2_1/c$
a (Å)	15.978(6)	7.574(4)	23.341(11)	14.061(6)
b (Å)	4.148(2)	11.662(6)	20.409(9)	11.917(5)
c (Å)	19.338(8)	33.970(19)	19.177(9)	17.848(7)
α (deg)	90	90	90	90
β (deg)	103.34(1)	90	90	105.58(1)
γ (deg)	90	90	90	90
V (Å^3)	1247.1(9)	3001(3)	9135(7)	2881(2)
Z	4	4	8	4
F(000)	712	1616	4992	1776
D_c (Mg m^{-3})	1.980	1.836	1.894	2.162
μ(Mo Kα) (mm^{-1})	4.20	3.50	4.57	5.43
temp (K)	300(2)	293(2)	299(2)	297(2)
cryst morphology	yellow platelet	yellow needle	colorless platelet	colorless platelet
cryst size (mm)	0.40 × 0.14 × 0.04	0.34 × 0.06 × 0.04	0.32 × 0.20 × 0.04	0.24 × 0.12 × 0.10
measd reflcns	14 404	24 839	33 473	32 431
unique reflcns	3521	5394	2764	8140
R_{int}	0.038	0.053	0.035	0.048
R_σ	0.047	0.047	0.014	0.056
$I > 2\sigma(I)$ reflcns	2298	4351	2583	4479
data/restr/params	3521/0/145	5394/44/296	2764/0/419	8140/0/298
GoF	$S(F^2) = 0.82$	$S(F^2) = 1.12$	$S(F^2) = 1.12$	$S(F^2) = 0.86$
FOM for $I > 2\sigma(I)$	$R(F) = 0.024$	$R(F) = 0.068$	$R(F) = 0.041$	$R(F) = 0.031$
	$wR(F^2) = 0.045$	$wR(F^2) = 0.148$	$wR(F^2) = 0.102$	$wR(F^2) = 0.053$
FOM for all data	$R(F) = 0.051$	$R(F) = 0.086$	$R(F) = 0.045$	$R(F) = 0.086$
	$wR(F^2) = 0.048$	$wR(F^2) = 0.154$	$wR(F^2) = 0.105$	$wR(F^2) = 0.061$
diff peak, hole (e Å^{-3})	0.42, −0.85	1.84, −3.06	0.86, −0.62	0.60, −0.66

[a] $R_{int} = \Sigma|F_o^2 - F_{mean}^2|/\Sigma|F_o^2|$; $R_\sigma = \Sigma|\sigma(F_o^2)|/\Sigma|F_o^2|$; $R(F) = \Sigma||F_o| - |F_c||/\Sigma|F_o|$; $wR(F^2) = [\Sigma w(F_o^2 - F_c^2)^2/\Sigma wF_o^4]^{1/2}$; $S(F^2) = [\Sigma w(F_o^2 - F_c^2)^2/(n - p)]^{1/2}$, with n number of reflections and p number of refined parameters; $w = 1/[\sigma^2(F_o^2) + (0.019P)^2 + 1.88P]$, where $P = (F_o^2 + 2F_c^2)/3$.

seemed necessary. Being that the glide plane *a* unambiguously confirmed by systematic absences, attempts were made to refine the structure in the nonisomorphic subgroup *Pa* of $Pna2_1$. No appreciable improvements were however obtained, so that $Pna2_1$ was definitely accepted. The disorder (46%) affecting one of its two independent organic ligands was modeled by superimposing two organic moieties almost related by a 180° rotation about their longest inertial axis (ligands 2A and 2B in Figure 2). Coincidence of chemically equivalent bond distances and angles was imposed. All atoms were assigned identical, but refinable, isotropic thermal parameters. No hydrogens were added.

The disorder affecting the *tert*-butylic groups of two organic ligands in compound **3** (ligands 3 and 4 of Figure 4 with disorder percentages of 18 and 25, respectively) was modeled by imposing the contemporaneous presence of two *tert*-butyls reciprocally tilted by 60°. Refinement was driven to completeness by assigning identical but refinable isotropic thermal parameters and imposing the coincidence of chemically equivalent bond distances. No hydrogen atoms were added. Further refinement details and crystal data are gathered in Table 1.

Crystallographic data (excluding structure factors) for the structures reported in this paper have been deposited with the Cambridge Crystallographic Data Centre as supplementary publication Nos. CCDC 261941, 261942, 261943, and 261944. Copies of the data can be obtained free of charge on application to CCDC, 12 Union Road, Cambridge CB2 1EZ, U.K. (fax (+44)1223 336-033; E-mail deposit@ccdc.cam.ac.uk).

Results and Discussion

Synthesis, X-ray Structure Determination, and Chemical Behavior. Compounds **1**−**6** were synthesized by straightforward methods, starting from either CuI dissolved in KI saturated aqueous solutions and the proper ligand or the complex $[CuI(pyridine)]_4$ by ligand exchange; compounds **7** and **8** were obtained by ligand exchange from $[CuX(pyridine)]_4$ (X = Cl, Br) (see Experimental Section).

For compounds **1**−**4**, suitable single crystals for X-ray diffraction were obtained. The structural motifs observed are somehow influenced by the nature of the *para*-substituents on the organic ligands.

In the *trans*-4-stilbazole adduct, $[CuI(trans\text{-}4\text{-}stilbazole)]_n$ (**1**), arrangement of the asymmetric units defines the well-known double-stranded "stair" motif (Figure 1). As already reported for $[CuI(4\text{-}acetylpyridine)]_n$[3] and for known $[CuI(L)]_n$ stairs,[13] the presence of a planar, pseudoaromatic nitrogen-donor ligand bound to the metal implies a certain distortion from an ideal stair, i.e. from orthogonal steps. The stair translation axis is parallel to the monoclinic one: the strands thus describe 2_1 degenerate helixes of pitch 4.15 Å; i.e., they are intrinsically chiral. The latter asymmetry is yet vanished by the overall centrosymmetric packing in the space group $P2_1/c$. Any copper atom is tetracoordinated (to three iodine atoms and the nitrogen of one ligand) in distorted tetrahedral stereochemistry. The three Cu−I vectors and the Cu−N one are comparable to those of known $[CuI(L)]_n$ stairs. Table 2 collects Cu−I, Cu−N, Cu···Cu, and I···I distances for both **1** and a pool of Cambridge Structural Database (CSD) retrieved stairs.[13] The Cu···Cu$^{\#1}$ diagonal distance (2.85 Å) is greater than the sum of the van der Waals radii

(13) The reported values result from a statistical analysis on the $[CuI(L)]_n$ stairs (L = nitrogen-based pseudoaromatic ligand) retrieved from the 2003 edition of the Cambridge Structural Database.

Table 2. Comparison between the Values of Cu−I, Cu−I$^{\#1}$, Cu−I$^{\#2}$, Cu−N, Cu···Cu, and I···I Distances in Compound [CuI(*trans*-4-stilbazole)]$_n$, **1**, and the Average Values of the Same Distances in Known [CuI(L)]$_n$ "Stairs" Retrieved from the 2003 Version of the CSDS

compd	Cu−I (Å)	Cu−I$^{\#1\,a}$ (Å)	Cu−I$^{\#2}$ (Å)	Cu−N(1) (Å)	Cu···Cu (Å)	I···I (Å)
1	2.62	2.69	2.66	2.04	2.85	4.47
[CuI(L)]$_n$ stairs	2.67	2.71	2.64	2.05	3.07	4.39

[a] Consult Figure 3 for the labeling scheme.

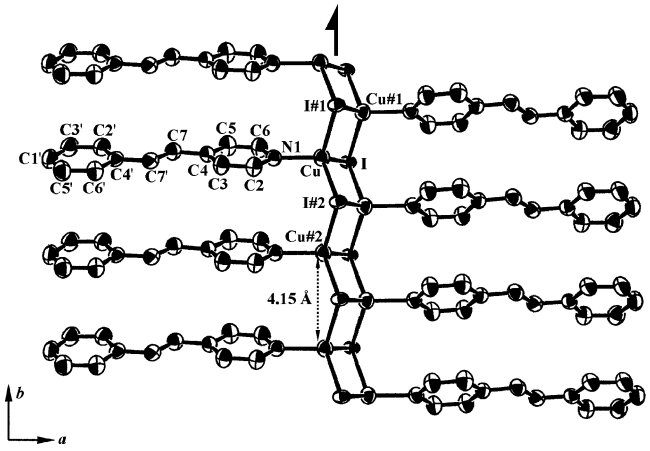

Figure 1. Representation, with 50% probability Ortep, of the double-stranded stair of compound [CuI(*trans*-4-stilbazole)]$_n$, **1**. Hydrogen atoms have been omitted for clarity. The labeling scheme adopted throughout the manuscript has been highlighted. The stair deviates from the ideality, i.e. from perfectly orthogonal steps. The stairs translation axes are parallel to *b*; i.e., the polymers evolve as degenerate 2_1 helices of pitch *b* (4.15 Å). The organic moieties stack on both sides of the strand with an interplanar distance of 4.15 Å (#1, $-x$, $y + 1/2$, $-z + 1/2$; #2, $-x$, $y - 1/2$, $z + 1/2$).

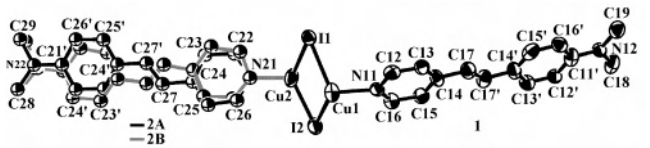

Figure 2. Representation, with 50% probability Ortep, of the dimeric [CuI(*trans*-4′-(dimethylamino)-4-stilbazole)]$_2$ asymmetric unit of compound [CuI(*trans*-4′-(dimethylamino)-4-stilbazole)]$_n$, **2**. Hydrogen atoms have been omitted for clarity. The labeling scheme adopted throughout the manuscript has been highlighted. Each metal coordinates two bridging halides and the nitrogen of a ligand. One of the independent ligands is affected by disorder (ca. 46%), modeled by superimposing two moieties (2A and 2B) related by a 180° rotation about their longest inertial axis.

(2.80 Å), as commonly (but not exclusively) happens in known [CuI(L)]$_n$ stairs. The halide is tricoordinated in distorted pyramidal geometry (diagonal I···I$^{\#1}$ = 4.47 Å vs an average of 4.39 Å of known stairs). The organic moieties approximately preserve their planarity and stack along both sides of the CuI skeleton, the distance between their mean planes being 4.15 Å.

Within the asymmetric unit of [CuI(*trans*-4′-(dimethylamino)-4-stilbazole)]$_n$ (**2**), each copper coordinates the nitrogen donor atom of one organic ligand, while the iodine atoms simply bridge two metal centers (Figure 2). The copresence of a 2_1 screw axis parallel to *a* and of a Cu−I bond between consecutive dimers creates a degenerate helicoidal strand of pitch *a* = 7.57 Å (Figure 3), a structural motif previously unknown for adducts of CuI of this kind. Along the polymeric unit, both copper and iodine experience two different coordination numbers: Cu(1) is tetracoordinated with a distorted tetrahedral geometry, while Cu(2) is tricoordinated with a planar trigonal stereochemistry. I(1)

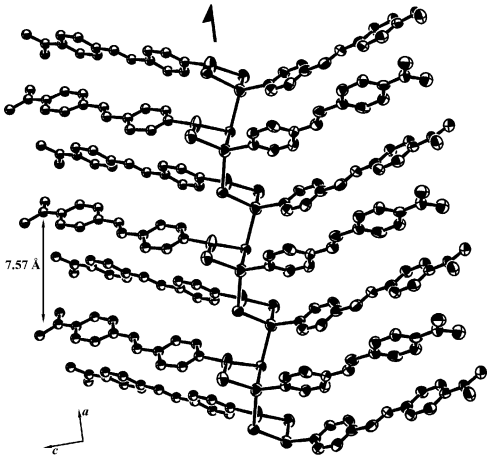

Figure 3. Representation, with 50% probability Ortep, of the structural motif of compound [CuI(*trans*-4′-(dimethylamino)-4-stilbazole)]$_n$, **2**. The absence of both hydrogen atoms and of the ligand 2A of the disordered model is due to clarity purposes. The polymer translation axis is parallel to *a*; the presence of Cu−I bonding interactions between consecutive dimers along this same axis results in an unprecedented degenerate helicoidal motif. The absence of stacking of consecutive ligands along both sides of the polymeric skeleton can be appreciated.

Table 3. Comparison, on the Basis of the Metal Coordination Number, between the Values of Geometrical Parameters Cu−I(1,2), Cu−N, and I(1)−Cu−I(2) in Compound [CuI(*trans*-4′-(dimethylamino)-4-stilbazole)]$_n$, **2**, and the Average Values for the Same Parameters in Known [CuI(L)$_n$]$_2$ (n = 1, 2) Dimers Retrieved from the 2003 Version of the CSDS

	Cu−I(1,2) (Å)		Cu−N (Å)		I(1)−Cu−I(2) (deg)	
Cu coord no.	2	[CuI]$_2$	2	[CuI]$_2$	2	[CuI]$_2$
3	2.55, 2.58	2.55, 2.57	1.99	2.00	123.9	118.7
4	2.62, 2.75	2.63, 2.65	2.05	2.07	114.7	110.5

and I(2) are tri and dicoordinated, respectively (Figure 3). Actually, both coordination number and stereochemistry influence Cu(1) and Cu(2) geometrical parameters. On going from the former to the latter, (i) Cu−I and Cu−N distances decrease and (ii) I−Cu−I angles increase (Table 3). Cu−I and Cu−N bond distances in **2** are comparable to the average values of Cambridge Structural Database retrieved [CuI(L)$_x$]$_2$ dimeric species (x = 1 or 2, Table 3).[14] In **2**, the metal···metal distance within a dimer (2.63 Å) is lower than the sum of the van der Waals radii (2.80 Å). In known [CuI]$_2$ dimers the latter distance undergoes a notable variety, spanning the 2.53−3.45 Å range, with a mean value of 2.85 Å.[14] As in most of the dimeric [CuI]$_2$ moieties, even in the present case the dimer is not planar: the angle between the planes described by the I(1)−Cu(1)−I(2) and I(1)−Cu(2)−I(2) triangles is about 14°. Both independent ligands ap-

(14) The reported values result from a statistical analysis on the [CuI(L)$_n$]$_2$ dimers (L = nitrogen-based pseudoaromatic ligand; n = 1, 2) retrieved from the 2003 edition of the Cambridge Structural Database.

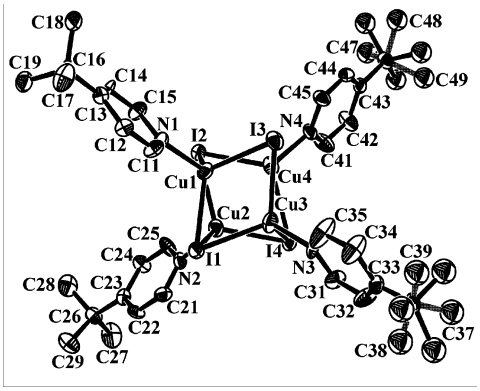

Figure 4. Representation, with 30% probability Ortep, of the tetrameric structural motif [CuI(4-*tert*-butylpyridine)]$_4$, **3**. Hydrogen atoms have been omitted for clarity. The labeling scheme adopted throughout the manuscript has been highlighted. A distorted tetrahedron of copper atoms is surrounded by a distorted tetrahedron of halogens. Each copper is tetracoordinated to three iodine atoms and the nitrogen of one organic ligand. The disorder affecting the substituents on ligands 3 and 4 (ca. 18 and 25%, respectively) has been modeled by imposing the contemporaneous presence of two *tert*-butylic moieties each, reciprocally tilted by 60°.

proximately preserve their planarity. As pointed out in the Experimental Section, one of them is affected by some orientational disorder (46%). As already shown for *trans*-stilbene and similar compounds,[15] this feature could be evidence of a local dynamic process comparable to a "pedal motion". The least-squares planes of the independent ligands are reciprocally tilted with respect to the Cu−Cu vector, thus forming an angle of ca. 66°. Interestingly, at variance with the "classical" [CuI(L)]$_n$ chains and stairs, no stacking of consecutive organic moieties is observed along the CuI skeleton: actually, along both sides, two distinct piles of ligands, having interplanar distance of 7.57 Å, are present (Figure 3).

The significant change of structural motif on going from **1** to **2** could be originated by the different steric hindrance of the ligands, which, in the latter compound, prevents their stacking on both sides of the CuI skeleton. To further strenghten this hypothesis, we synthesized the CuI adduct with 4′-*tert*-butyl-4-stilbazole (**5**). Concomitantly, to investigate the role of the length of the π-delocalized "bridge" on the structural motif, we prepared the CuI adduct with *trans*-4-[4-(4-(dimethylamino)phenyl)buta-1,3-dienyl]pyridine (**6**). Both derivatives were characterized by elemental analysis and ^{1}H NMR, but unfortunately we were unable to obtain suitable single crystals for X-ray diffraction.

When we shifted toward adducts of CuI with *para*-substituted derivatives of pyridine, we found, with 4-*tert*-butylpyridine, a structural motif unaltered (**3**) with respect to [CuI(pyridine)]$_4$: a distorted tetrahedron of copper atoms is included in a larger I_4 tetrahedron, whose vertexes cap the triangular faces of the Cu_4 polyhedron (Figure 4). The fourth coordination site of each Cu is occupied by a 4-*tert*-butylpyridine ligand. Average Cu−I, Cu−N, Cu···Cu, and I···I distances are in good agreement with those of known [CuI(L)]$_4$ tetramers (2.70, 2.04, 2.72, and 4.48 Å vs averages of 2.75, 2.05, 2.69, and 4.48 Å, respectively; Table 4).[16] Notably, the average Cu···Cu distance of **3** is shorter than the sum of the van der Waals radii (2.80 Å). As depicted by the thermal ellipsoids of Figure 4, the aromatic rings undergo a conspicuous thermal motion about the normal to their mean planes. *tert*-Butyl moieties as well are characterized by a high degree of motion. For ligands 3 and 4 (Figure 4) the latter is so pronounced to require a disordered model, according to which two *tert*-butyl groups, reciprocally tilted by 60°, have been contemporarily refined (see Experimental Section). Probably, the *tert*-butyl group in the *para* position hinders the stabilization of the polymeric stair structure, easily formed with the "naked" pyridine. However, by emission studies, we had evidence of the presence, in the reaction mother liquor, of a very minor amount of the polymeric stair form of **3** (see Experimental Section).

Table 4. Comparison between the Average Values of Cu−I, Cu−N, Cu···Cu, and I···I Distances in Compound [CuI(4-*tert*-butylpyridine)]$_4$, **3**, and in Known [CuI(L)]$_4$ Tetramers Retrieved from the 2003 Version of the Cambridge Structural Database

compd	⟨Cu···Cu⟩ (Å)	⟨I···I⟩ (Å)	⟨Cu−I⟩ (Å)	⟨Cu−N⟩ (Å)
3	2.72	4.48	2.70	2.04
[CuI(L)]$_4$ tetramers	2.69	4.48	2.75	2.05

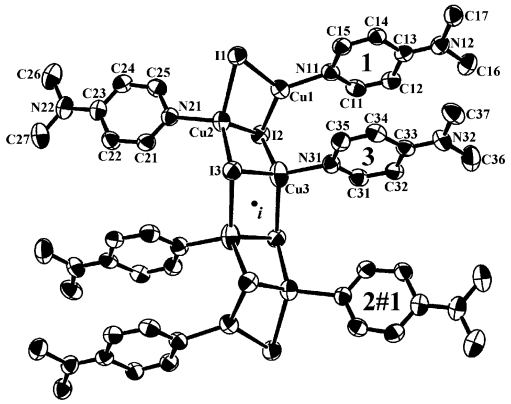

Figure 5. Representation, with 50% probability Ortep, of the hexameric structural motif in [CuI(4-dimetilaminopyridine)]$_6$, **4**. Hydrogen atoms have been omitted for clarity. The labeling scheme adopted throughout the manuscript has been highlighted. The hexamer reminds the distorted portion of a stair, the distortion implying absence of complete stacking of the ligands on both sides of the CuI skeleton (angles between the average planes of ligands 1/3 and 3/2$^{\#1}$ of 6 and 68°, respectively) (#1, $-x$, $-y$, $-z$).

By substitution of the *tert*-butyl group with a dimethylamino group (**4**), characterized by significantly different electronic properties and by a minor steric hindrance, the structural motif is strongly affected. Structure solution of **4** revealed the first example of a hexameric [CuI(L)]$_6$ oligomer (L = (dimethylamino)pyridine) (Figure 5), which could be viewed as a "cut" portion of a stair. Among the consequences of the cut, it is worth noting the loss of complete stacking of the ligands: on both sides of the CuI skeleton, just ligands 1 and 3 (Figure 5) are approximately piled (acute angle between their least-squares planes 6.3°); the average plane

(15) Galli, S.; Mercandelli, P.; Sironi, A. *J. Am. Chem. Soc.* **1999**, *121*, 3767 and references therein.

(16) The reported values result from a statistical analysis on the [CuI(L)]$_4$ tetramers (L = nitrogen-based pseudoaromatic ligand) retrieved from the 2003 edition of the Cambridge Structural Database.

Table 5. Comparison between the Average Values of Cu−I, Cu−N, Cu···Cu, and I···I Distances in Compound $[Cu_3I_3(4\text{-dimethylaminopyridine})_3]_2$, **4**, and in Known $[CuI(L)]_n$ Stairs Retrieved from the 2003 Version of the Cambridge Structural Database

compd	⟨Cu−I⟩ (Å)	⟨Cu−N⟩ (Å)	⟨Cu···Cu⟩ (Å)	⟨I···I⟩ (Å)
4	2.65	2.01	2.84	4.46
$[CuI(L)]_n$ stairs	2.67	2.05	3.07	4.35

of ligand $2^{\#1}$ is tilted by 68.0° with respect to that of 3. Mean Cu···Cu and I···I diagonal interactions and mean Cu−I and Cu−N bond distances have values of 2.84, 4.46, 2.65, and 2.01 Å, respectively. The quoted figures support the interpretation of **4** as a distorted portion of a stair; actually, known $[CuI(L)]_n$ stairs show average Cu···Cu and I···I diagonal interactions of 3.07 and 4.35 Å and, particularly, Cu−I and Cu−N bond distances of 2.67 and 2.05 Å, respectively (Table 5).[13]

These latter two structures, together with the CuI adduct with *para*-cyanopyridine,[17] clearly add further evidence that even in the case of simple ligands such as pyridine, the *para*-substituent on the organic ligand can influence the structural motif by its steric (*tert*-butyl), electronic/steric (dimethylamino), or bridging-donor (cyano) properties, with disruption of the stair structural motif.

Probably due to their intrinsic instability toward oxidation, we could not obtain suitable single crystals of **7** and **8** for X-ray diffraction. However, X-ray powder diffraction showed that they are not isomorphous to **2**. Furthermore, the lack of second harmonic generation under the Kurtz−Perry experimental conditions (see below) prompts, differently from **2**, a centrosymmetric crystallographic arrangement. This seems to suggest that even the nature of the bridging halides, not just that of the organic moiety, may play a nonnegligible role in the definition of the structural motif.

It is worth mentioning that, during the synthesis of **2**, traces of [CuI(*cis*-4′-(dimethylamino)-4-stilbazole)] (**2′**) formed, as evidenced by ^{1}H NMR spectroscopy. To check for a possible influence of the *cis*:*trans* conformation of the ligand on the structural motif, we tried to prepare pure **2′** from **2** irradiated with a 125 W Hg/Xe lamp. In this regard, we observed that although irradiation of **2** in CH_3CN allows the formation of good amounts of **2′**, the latter is obtained in much better yield (^{1}H NMR evidence) by photoisomerization of *trans*-4′-(dimethylamino)-4-stilbazole in CH_2Cl_2, followed by exchange reaction with $[CuI(pyridine)]_4$ in CH_2Cl_2. Unfortunately, various attempts to prepare suitable single crystals of **2′** invariably failed; however, the proof of its belonging to a noncentrosymmetric space group came from a not nihil SHG signal (see below). Interestingly, contrarily to **2**, the related compounds **1**, **5**, and **6**, carrying a *trans*-stilbazolic ligand as well, and the CuCl (**7**) and CuBr (**8**) adducts of *trans*-4′-(dimethylamino)-4-stilbazole, much more easily oxidized by air to Cu(II) species, did not present evidence for a *trans* to *cis* isomerization of their ligands during their preparation.

(17) Graham, A. J.; Healy, P. C.; Kildea, J. D.; White, A. H. *Aust. J. Chem.* **1989**, *42*, 177.

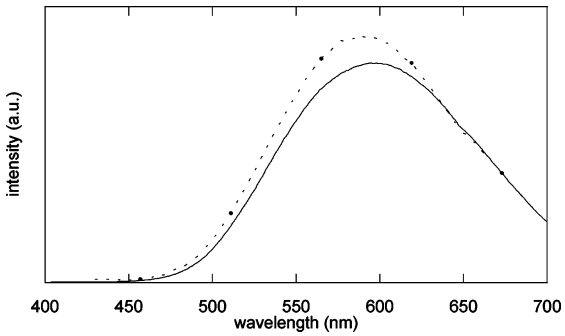

Figure 6. Solid-state emission spectra of compounds **3** and **4** (continuous and dotted lines, respectively). In the case of **4** the spectrum has been magnified (1.5×) for the sake of clarity.

Table 6. Positions of Solid-State Emission Maxima for Compounds $[CuI(trans\text{-4-stilbazole})]_n$, **1**, $[CuI(trans\text{-4′-(dimethylamino)-4-stilbazole})]_n$, **2**, $[CuI(4\text{-}tert\text{-butylpyridine})]_4$, **3**, $[Cu_3I_3(4\text{-(dimethylamino)pyridine})_3]_2$, **4**, $[CuI(pyridine)]_n$, $[CuI(3\text{-methylpyridine})]_n$, $[CuI(4\text{-methylpyridine})]_n$, $[CuI(4\text{-acetylpyridine})_2]_n$, and $[CuI(4\text{-acetylpyridine})]_n$

compd	λ_{max}^{em} (nm)	ref
$[CuI(trans\text{-4-stilbazole})]_n$, **1**	quenching	this work
$[CuI(trans\text{-4′-(dimethylamino)-4-stilbazole})]_n$, **2**	quenching	this work
$[CuI(4\text{-}tert\text{-butylpyridine})]_4$, **3**	452, 602	this work
$[Cu_3I_3(4\text{-(dimethylamino)pyridine})_3]_2$, **4**	580	this work
$[CuI(pyridine)]_n$	437	2
$[CuI(3\text{-methylpyridine})]_n$	454	4
$[CuI(4\text{-methylpyridine})]_n$	437	4
$[CuI(4\text{-acetylpyridine})_2]_n$	612	3
$[CuI(4\text{-acetylpyridine})]_n$	700	3

Photoluminescent Emission Studies and Solid-State Second-Order NonLinear Optical Properties. Table 6 reports the emission maxima positions (λ_{em}^{max}) for compounds **1**−**4**. For comparison, λ_{em}^{max}'s of $[CuI(pyridine)]_n$, $[CuI(3\text{-methylpyridine})]_n$, $[CuI(4\text{-methylpyridine})]_n$, $[CuI(4\text{-acetylpyridine})_2]_n$, and $[CuI(4\text{-acetylpyridine})]_n$ are reported as well.

First we investigated the behavior of the CuI adducts **3** and **4**, with the two *para*-substituted pyridines studied in this work. The room-temperature solid-state photoluminescence spectrum of **3** (see Figure 6) shows a broad, bright yellow, structureless emission, centered at 602 nm.[18] Solid-state photoluminescent behavior of CuI tetramers have been systematically analyzed.[2] Their yellow emission (centered around 580−625 nm) has been interpreted as a decay from a triplet "cluster centered" (^{3}CC*) excited state; the latter involves both the I_4 and Cu_4 tetrahedra and has mixed halide-to-metal charge transfer (^{3}XMCT*) and "metal cluster centered" [^{3}MCC*, $d_{Cu} \rightarrow (s,p)_{Cu}$] characters. The emission of **3** can be undoubtedly considered a decay from a ^{3}CC* excited state, the existence of a ^{3}MCC* contribution being supported by a Cu···Cu nonbonding interaction of 2.72 Å. Although the structural motif of **4** was neither reported nor photophysically studied before, its emission, characterized by a LE maximum at 580 nm (see Figure 6), can be

(18) It is worth mentioning that occasionally a very weak blue emission centered at 452 nm is also observed. This weak high-energy HE emission can be due to the presence of a minor amount of the polymeric chain adduct, since the solid-state room-temperature emission of these polymers is reported to be centered at about 430−460 nm.[2]

tentatively attributed, as for the adducts with a chain or stair polymeric network,[3] to a ^{3}XLCT* excited state. Moreover, the Cu···Cu distance of 2.84 Å, higher than the sum of the van der Waals radii (2.80 Å), allows discarding any contribution from excited states involving metal-delocalized orbitals. However, a ^{3}MLCT* process cannot be excluded.[3]

Rather surprisingly, the room-temperature solid-state emission spectra of both **1** and **2** show no luminescence. The structural motif of **2** was previously unknown in the literature, so that no preexisting models are at hand to discuss its emissive properties: the only available clue is its Cu···Cu diagonal distance (2.63 Å), shorter than the sum of the van der Waals radii, which would anticipate the possible participation of ^{3}MCC* contributions to the emission process. At variance, being **1** is a typical stair with a Cu···Cu distance (2.85 Å) higher than the sum of the van der Waals radii, a HE emission of the ^{3}XLCT* type is expected.[2] The stairs for which a HE emission was reported ([CuI(pyridine)]$_n$, [CuI(3-methylpyridine)]$_n$, [CuI(4-methylpyridine)]$_n$, and [CuI-(4-acetylpyridine)]$_n$) are characterized by ligands of *pyridinic* type. Significantly, even within this limited pool of ligands, a nonnegligible effect of their electronic properties on the emission maxima energy was already noticed.[3] In light of this, being the metal and the halide in **1** are identical with those in the above pyridinic stairs, the presence, in **1**, of *trans*-stilbazole inevitably drives the attention on the role of π-conjugation extension.

The more extended π-conjugation of *trans*-stilbazole may be the key factor in making quenching of luminescence effective. Intermolecular interactions of π-delocalized molecules, in the solid state, have been already invoked to explain the process of luminescence quenching. Actually, calculations carried out on cofacial stilbenic arrangements have shown that, for intermolecular distances above 8 Å, there is no exciton transfer between the two π electronic systems, which behave as separate entities, as in solution.[19] However, by a decrease of the intermolecular distance below the critical value of 7 Å, the mixing of HOMO and LUMO orbitals produces excited states characterized by a potentially reduced efficiency of the emission process. Indeed, the stair adduct of *trans*-stilbazole with CuI, **1**, where the organic moieties stack at a distance of only 4.15 Å, does not emit at all. The quenching of the emission process could possibly be due to an extensive HOMO and LUMO orbital mixing of π systems closely interacting. Quite unexpectedly, there is no evidence even for the emission typical of a CuI stair network, attributed to a ^{3}XLCT excited state.[2] More probably, then, the quenching of the emission involves a mixing of the π systems of *trans*-stilbazoles and of orbitals delocalized on the CuI skeleton: a nonemissive ^{3}MLCT, for example, could be at work. This hypothesis is confirmed by the solid-state emission spectrum of *trans*-stilbazole itself, which shows an intense emission in the blue spectral region plus a broad and much weaker band in the 500−700 nm region. The latter, which is absent in solution emission spectra of stilbazole, is probably originated by intermolecular interactions present in the solid state,[20] where the π systems stack at a distance of 6.33 Å, *below* the critical value proposed by Bredas.[19] Noteworthy, in acetone solution, the emission spectrum of **1** shows a maximum at 420 nm, not too different from that of the free ligand. This could be due to lability in solution of the stilbazolic ligands in this kind of Cu(I) complexes, as evidenced by the broad ^{1}H NMR signals of H_2 and H_6 (see Experimental Section).

In the case of **2**, in the solid state, an emission quenching process takes place even if the consecutive *trans*-stilbazolic moieties stack at a distance of 7.57 Å, *above* that for any relevant interligand π interaction.[19] On the contrary, *trans*-4′-(dimethylamino)-4-stilbazole itself, whose moieties are stacked at a distance similar to that in **2** (7.66 Å)[21] shows, in its solid-state emission spectrum, two peaks at 477 and 503 nm. Moreover, as for **1**, any additional emission which can be attributed to the CuI polymeric network is completely lacking (on the basis of the rather short Cu···Cu distance, 2.63 Å, a ^{3}MCC* contribution to the emission involving the Cu skeleton, could be expected[2]). The inadequate distance for significant interligand $\pi-\pi$ interactions to be at work, supports, even for **2**, the role, in the quenching process, of orbitals belonging to the CuI skeleton. A nonemissive ^{3}MLCT, e.g., cannot thus be discarded. As observed for **1**, also in the case of **2**, an emission process is restored in acetone solution, with a maximum centered at 468 nm and a shoulder at 500 nm, analogous to the emission, in the same solvent, of the free *trans*-stilbazolic ligand.

Similar is the behavior of **5**, with total quenching of the emission in the solid state and emission at 412 nm in acetone solution. Since for **5** the structural motif is not available, we cannot explain its solid-state quenching on a structural basis. Due to the larger steric hindrance of the *tert*-butyl group with respect to the dimethylamino one, we may argue that the polymeric motif of the stair is unlikely. The above evidence strongly suggests that, when a *trans*-stilbazolic ligand is bound to a polymeric CuI skeleton, complete solid-state quenching occurs of the expected emissions of both the *trans*-stilbenic moiety and the CuI skeleton (the latter involving either a ^{3}XLCT* or a ^{3}MCC* excited state). We have evidence that the quenching process probably does not take place only through space, between the adjacent π delocalized systems of *trans*-stilbazoles, but involves a mixing of the excited states of adjacent π-delocalized *trans*-stilbazoles with excited states located mainly or partially on the polymeric CuI skeleton.

As a final confirmation to this hypothesis, we have found that in the case of compound **6**, with an even more π delocalized ligand and therefore π* excited states of lower energy, the solid-state emission is not totally quenched. A relatively weak emission is indeed observed at 580 nm, while the free ligand shows, in the solid state, a strong emission at 540 nm with a shoulder at 565 nm. The presence of a weak, in **6**, emission is in agreement with the reported

(19) Cornil, J.; dos Santos, D. A.; Crispin, X.; Silbey, R.; Bredas, J. L. *J. Am. Chem. Soc.* **1998**, *120*, 1289.

(20) Cariati, E.; Roberto, D.; Ugo, R.; Srdanov, V. I.; Galli, S.; Macchi, P.; Sironi, A. *New J. Chem.* **2002**, *26*, 13.

(21) Lacroix, P. G.; Daran, J. C.; Nakatani, K. *Chem. Mater.* **1998**, *10*, 1109.

decreased effect on the emission quenching by increasing the length of π delocalized systems.[19] As in the other cases, in acetone solution, the emission spectrum of **6** shows an emission band centered at about 550 nm quite similar to that of the free ligand in the same solvent. Unfortunately, even for **6** we have not been able to grow single crystals suitable for X-ray structural characterization.

Testing the second harmonic generation (SHG) efficiencies on unsieved powders of **1**−**8** via the Kurtz−Perry powder method[9] working with an incident wavelength of 1.064 nm, resulted in lack of SHG not only for **1**, **3**, and **4** (as expected because of their well-established centrosymmetric space groups) but also for **5**−**8** thus suggesting at least a centrosymmetric space group. Only **2** has shown a discrete SHG with efficiency of 22.5 times that of quartz. A comparable SHG efficiency has been observed also for a mixture of **2′**and **2** with a ratio of 13:1.

As described by the "two-level model",[22] the *molecular* second-order NLO response of organic and, to a lesser extent, organometallic species, can be retraced to one prevailing charge transfer (CT) process. In the *solid state*, this contribution is "tuned" by the reciprocal arrangement of the molecular entities. This concept was successfully tackled by Zyss,[23] who eventually proposed a set of geometrical relationships linking the molecular quadratic hyperpolarizability along the CT axis (β_{CT}) to the crystalline nonlinearity/molecule (b_{eff}).

Thus, in the presence of such a performing chromophore as *trans*-4′-(dimethylamino)-4-stilbazole, we tried to explain the poor SHG efficience of species **2** by taking advantage of the geometrical model developed by Zyss. The latter was applied (i) adopting an "oriented gas" model, i.e. supposing that the chromophores interact only weakly, (ii) assuming, at first approximation, that SHG active moieties can be described by a monodimensional system whose axis coincides with the CT direction, and (iii) identifying the CT axis with the longest inertial axis of the *trans*-4′-(dimethylamino)-4-stilbazole chromophore, i.e. with the N···N vector.

According to the crystallographic class of **2**, *mm*2, the two phase matchable components of b_{eff} have expression $b_{ZXX} = \sin^2(\phi)\cos(\theta)\sin^2(\theta)\beta_{CT}$ and $b_{ZYY} = \cos^2(\phi)\cos(\theta)\sin^2(\theta)\beta_{CT}$, where θ and ϕ are the angles between the assumed CT axis and *c*, and between the projection of the CT axis on *ab* and a, respectively. The ratios b_{ZXX}/β_{CT} and b_{ZYY}/β_{CT} reach their optimum value of 0.385 for $\theta = 54.74°$ and $\phi = 90°$ or 0°, respectively. In **2**, the actual values of θ and ϕ are −14.89 and 75.12° or 15.15 and 74.86° for the two independent ligands (L1 or L2), unfavorably directed toward almost opposite directions with respect to *c*. An overall $b_{eff} = |(b_{ZXX}/\beta_{CT} + b_{ZYY}/\beta_{CT})_{L1} - (b_{ZXX}/\beta_{CT} + b_{ZYY}/\beta_{CT})_{L2}|$ value of $|(0.060 + 0.004)_{L1} - (0.0061 + 0.004)_{L2}| = 0.001$ results. The SHG performance of **2** is thus about 4% of the optimum predicted by Zyss' model, this allowing an explanation of the modest SHG signal detected.

Conclusions

CuI adducts with a series of *para*-substituted *trans*-stilbazoles and pyridines show a rich structural behavior. In particular, the introduction of a dimethylamino group in the *para*-position either of a *trans*-stilbazolic moiety or of a pyridine ring produces two new structural motifs. The polymeric helicoidal motif of compound [CuI(*trans*-4′-(dimethylamino)-4-stilbazole)]$_n$, totally new, arranges in a noncentrosymmetric crystal structure and affords a discrete SHG when irradiated at 1064 nm. Differently from pyridines,[2] to rationalize the solid-state photoemission behavior of CuI adducts with *para*-substituted *trans*-stilbazoles, the structural motif cannot be considered the only parameter to be taken into consideration. In these latter adducts, any solid-state photoemission originated either from the π system of the *trans*-stilbazolic moiety or from the CuI skeleton is unexpectedly quenched, both totally (as in the case of [CuI(*trans*-4-stilbazole)]$_n$, [CuI(*trans*-4′-(dimethylamino)-4-stilbazole)]$_n$, and [CuI(4′-*tert*-butyl-4-stilbazole)]$_n$) or partially (as in the case of [CuI(*trans*-4-[4-(4-(dimethylamino)phenyl)-buta-1,3-dienyl]pyridine]). On the basis of the different arrangement of the *trans*-stilbazolic moieties in the crystalline structures of **1** and **2** (Figures 1 and 2), the quenching seems not to be due only to a mixing of their π HOMO and LUMO levels, but probably it involves mixing of the level of π^* excited states of the organic ligands and orbitals of the CuI skeleton (^{3}XLCT* or ^{3}MCC*).

In conclusion, we have produced an unexpected evidence for a surprising quenching of the photoemission process in hybrid inorganic−organic materials such as adducts between CuI and a series of *trans*-stilbazoles.

We have also evidenced a specific role of the dimethylamino group, when located in *para* position to a pseudo-aromatic (pyridine) or aromatic (the phenyl group of a *trans*-stilbazolic moiety) ligand, in producing new and unusual structural motifs of the CuI skeleton either polymeric or oligomeric.

Acknowledgment. This work was supported by the Ministero dell'Istruzione, dell'Università e della Ricerca (Programma di ricerca FISR 2001; research title "Nanotecnologie molecolari per l'immagazzinamento e la trasmissione delle informazioni: Nanotecnologie per la comunicazione ottica"). We deeply thank Dr. Francesca Tessore and Dr. Maurizio Gallina for experimental help and Mr. Pasquale Illiano for NMR measurements. We also acknowledge one of the reviewers for his fruitful comments.

Supporting Information Available: X-ray crystallographic data in CIF format. This material is available free of charge via the Internet at http://pubs.acs.org.

IC050143S

(22) (a) Oudar, J. L.; Chemla, D. S. *J. Chem. Phys.* **1977**, *66*, 446. (b) Oudar, J. L. *J. Chem. Phys*. **1977**, *67*, 2664.

(23) (a) Zyss, J.; Oudar, J. L. *Phys. Rev. A* **1982**, *26*, 2028. (b) Zyss, J.; Chemla, D. S. In *Nonlinear Optical Properties of Organic Molecules and Crystals*; Chemla, D. S., Zyss, J., Eds.; Academic Press Inc.: Orlando, FL, 1987; Vol. 1, pp 23−187.